J Mater Sci (2011) 46:1272–1280
DOI 10.1007/s10853-010-4911-8

Effect of composition on fracture behavior of polypropylene–wollastonite–polyolefin elastomer system

Zhuo Fu · Wenli Dai · Haimei Yu · Xiaoxuan Zou · Baiquan Chen

Received: 20 May 2010 / Accepted: 7 September 2010 / Published online: 22 September 2010

Abstract The fracture behavior of polypropylene (PP)–wollastonite–polyolefin elastomer (POE) in the mixed mode region was studied using the essential work of fracture (EWF) method. The relationship between the microstructure and the fracture parameters was analyzed. The effect of wollastonite content on the essential work of fracture and the work of plastic deformation was discussed. The energy dissipation during a double-edge-notched tension (DENT) test was calculated with the EWF method. It was found in the mixed mode region that σ_n increases with shortening of the ligament length region as plastic constraint effect rises and variation of the specific total work of fracture with ligament length was still reasonably linear within the mixed mode region. With increasing wollastonite content, w_e (specific essential work of fracture) increases, while the βw_p (specific non-essential work of fracture) decreases. The measurements of energy dissipation show that improvement in the fracture toughness of PP–wollastonite–POE is mainly due to the increase in crack propagation resistance during the necking and tearing processes after yielding, while the plastic deformation capability of the material depends mainly on the properties of fracture behavior before yielding. It is also found that the impact strength of the material decreases with increasing wollastonite content. However, the composition with high impact strength has lower specific essential energy of fracture and lower long-term fracture resistance, indicating that EWF is a better indicator of long-term fracture properties than the impact strength. DSC results show that the presence of wollastonite hinders crystallization of the PP.

Z. Fu (✉) · W. Dai · X. Zou
Department of Polymer Science and Engineering, Institute of Chemistry, Xiangtan University, Xiangtan, China
e-mail: fuzhuo80@126.com

Z. Fu · W. Dai · H. Yu
Key Laboratory of Advanced Functional Polymeric Materials, College of Hunan Province, Xiangtan University, Xiangtan, China

B. Chen
Key Laboratory of Polymeric Materials and Application Technology, Xiangtan University, Xiangtan, Hunan Province, China

Introduction

Polypropylene (PP) is a material widely used in various industries, due to its abundance, low price, easy molding, and good overall properties. It has become one of the fastest developing materials among common resins. However, PP has low strength and low hardness. It becomes brittle at low temperatures. It has large shrinkage during molding, easily decomposes and ages, and has low thermal resistance. Large effort has been made to improve the properties of PP for wider application. Introduction of inorganic particles into PP has been shown to improve the fracture toughness of the material [1–4].

In order to characterize the fracture behavior of ductile polymeric materials, a theory called the essential work of fracture (EWF), originally proposed by Broberg [5], has been widely used by many authors [6–13]. In this theory, the deformation at the crack tip is divided into an inner fracture process zone (IFPZ) and an outer plastic deformation zone (OPDZ), as shown in Fig. 1. The energy required for the fracture in the IFPZ is called the essential work of fracture, W_e, and the energy required for the deformation in the OPDZ is called the non-essential work of fracture, W_p. The total work of fracture, W_f is given by:

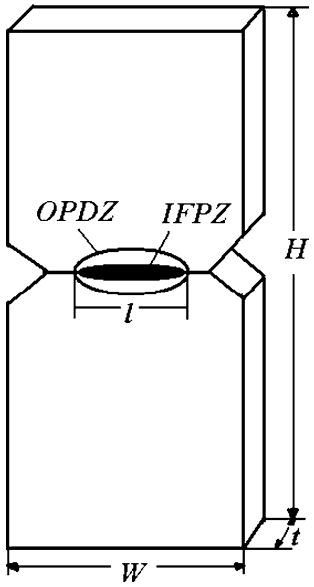

Fig. 1 Illustration of a DENT specimen

$$W_f = W_e + W_p. \quad (1)$$

When both IFPZ and OPDZ are present in the ligament, W_e is the energy used in the IFPZ to form a neck and the subsequent tearing. It is a surface energy term that is proportional to ligament area, i.e.,

$$W_e = w_e l t, \quad (2)$$

where w_e is called the specific essential work of fracture, l is the ligament length, and t is the specimen thickness.

The energy consumed in the OPDZ, W_p, is assumed to be proportional to the volume of the yielded zone, i.e.,

$$W_p = \beta w_p l^2 t, \quad (3)$$

where β is a geometric constant depending on the shape of the specimen and the crack, w_p is called the specific non-essential work of fracture.

Combining Eqs. 1–3 gives:

$$w_f = W_f/lt = w_e + \beta w_p l, \quad (4)$$

where w_f is termed as the specific total work of fracture. Equation 4 shows that w_f has a linear relationship with ligament length. The slope and y-intercept are βw_p and w_e, respectively.

The specific total work of fracture w_f can be divided into two terms: w_y, the specific total work of fracture for yielding, and w_n, the specific total work of fracture for necking and tearing, i.e.,

$$w_f = w_y + w_n, \quad (5)$$

Similar to Eq. 4, terms w_y and w_n can be expressed as:

$$w_y = w_{e,y} + \beta' w_{p,y} l, \quad (6)$$

$$w_n = w_{e,n} + \beta'' w_{p,n} l, \quad (7)$$

where $w_{e,y}$ and $w_{e,n}$ are the yielding and the necking terms of the specific essential work of fracture, respectively, and $\beta' w_{p,y}$ and $\beta'' w_{p,n}$ the yielding and the necking terms of the non-specific essential work of fracture, respectively.

This work introduced the polyolefin elastomer (POE) and wollastonite into PP to improve the fracture toughness of the PP material and studied the fracture behavior of the PP–wollastonite–POE composite using the EWF theory. Except for very thin plates, most of the plates are in the plane-stress/plane-strain transition region. Therefore, it is important for researchers to study the behavior of materials in the plane-stress/plane-strain transition region. Linear elastic fracture mechanics is not suitable for ductile materials. J-integral method has strict requirement on the dimensions of specimens and only applies to thick specimens. This work tried to study the fracture behavior of ductile materials in the plane-stress/plane-strain transition using the EWF theory. The plane-stress fracture [14, 15] is expected to occur when the ligament length l and width w satisfy $3t \leq l \leq w/3$, while the plane-strain fracture [16, 17] occurs when $l \leq t$. The dimension of the specimens used in this study follows $t < l < 3t$ and thus fall into the plane-stress/plane-strain transition region. Researchers have proposed various ways to treat the data in this region, such as power [18] or linear curve fitting [19–22]. This work tried to study the fracture parameters of PP–wollastonite–POE material as a function wollastonite and POE contents through microstructure change and used the linear relationship to derive the fracture parameters in the transition region.

Experimental

Materials and sample preparation

The raw materials used in this study were PP (H045, Hunan Changsheng Petrochemicals, Ltd.), wollastonite (1250 grit, NEW-XA800, Xinyu Nanfang Wollastonite Industries Co.), and POE (TAFMER™ Alpha-olefin copolymer, Mitsui Elastomers Singapore Pte Ltd.). The raw materials were mixed according to the designated ratios as shown in Table 1 and granulated in a twin-screw extruder (SJSH-30, Nanjin Rubber and Plastic Machinery Factory), with

Table 1 Composition of the PP–wollastonite–POE

Sample	PP (wt%)	Wollastonite (wt%)	POE (wt%)
A	92	0	8
B	82	10	8
C	72	20	8
D	62	30	8
E	100	0	0

temperature profiles between 160 and 210 °C. The resulting pellets were dried and then injected using an injection-molding machine (HTB-80, Ningbo Haitian Plastic Machinery Co.) into 4-mm thick dumbbell-shaped and rectangular specimens. The temperatures from the feed zone to the nozzle were 190, 200, 230, and 220 °C. The injection and the holding pressures were both 50 MPa. The injected specimens were cut into 63 mm × 10 mm × 4 mm DENT specimens according to Fig. 1. The free ligament length was between 4 and 8 mm. The edge notches were cut by a blade. The specimen dimension was measured with a caliper, and the notch length was measured using an optical microscope.

Material characterization

The load–displacement curves of the DENT specimens were measured using a universal test machine (RGT-10, Shenzhen Ruiger Instruments Ltd.) at room temperature (23 ± 2 °C). The crosshead speed for the DENT test was 10 mm/min. The gauge length of the specimen was about 32 mm. The maximum net stress (σ_{net}) is obtained by dividing maximum load by lt. The uniaxial tensile yield stress, σ_y, was measured from the load–displacement curves of the dumbbell-shaped specimens with a crosshead speed of 50 mm/min and a gauge length of 70 mm.

The impact strength of the samples was measured using a Charpy v-notched test machine (XJU-22 Chengde Jinjian Testing Instrument Co., Ltd.). The cross-sectional dimensions of the specimen were 8 × 4 mm.

The melting behavior and crystallization dynamics of the materials were studied using a Differential Scanning Calorimetry (DSC, PE Q10). The sample was heated from 30 to 200 °C at 20 °C/min and then cooled to 30 °C at 10 °C/min in a nitrogen atmosphere.

Results and discussion

Load–displacement curves

Figure 2 shows the load–displacement curves of DENT specimens with a ligament length of 7 mm. For PP–wollastonite–POE, the specimen yields as load reaches a certain level and starts necking until the specimen broke. All specimens failed in a ductile manner and their load–displacement curves exhibit geometrical similarity, satisfying an essential pre-requisite of the EWF theory.

Fracture toughness and EWF parameters

Following the Hill's predictions, the pure plane-stress solicitation of a DENT specimen gives a σ_{net} value of $1.15\sigma_y$, which rises to $2.97\sigma_y$ in pure plane-strain conditions.

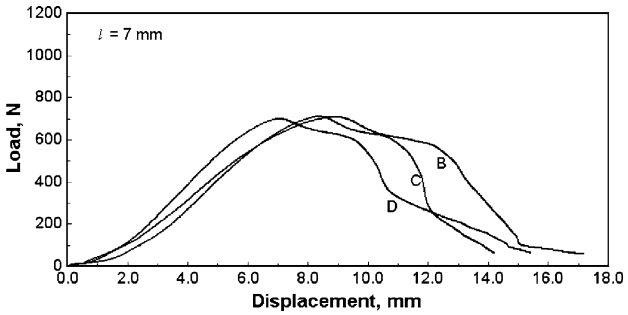

Fig. 2 Typical load–displacement curves of PP–wollastonite–POE with various mass ratio: (*B*) 82/10/8; (*C*) 72/20/8; (*D*) 62/30/8

It can be seen from Figs. 3, 4, and 5 that the σ_n does not equal to $1.15\sigma_y$, because the specimen is not in the plain-stress region, but rather in the mixed-mode region. It was found in the mixed-mode region that σ_n increases with shortening of the ligament length region as plastic constraint effect rises and variation of the specific total work of fracture with ligament length was still reasonably linear within the mixed-mode region.

The specific total work of fracture (w_f) and its contributing terms (w_y and w_n) were calculated from the corresponding portions of the load–displacement curves. Figures 6, 7, and 8 show the values of w_f, w_y, and w_n as a function of the ligament length for samples B–D, exhibiting good linear relationships for all the samples and meeting the conditions of the EWF theory.

Figure 9 shows the values of w_e, $w_{e,y}$, and $w_{e,n}$ as function of wollastonite content. It can be seen that with increasing wollastonite content, the w_e values of the blends increases significantly, indicating the significant improvement in the fracture toughness of the material. This implies that the addition of wollastonite into the PP–POE material improves the resistance to crack propagation of the material. However, the specific non-essential work of fracture (βw_p) decreases with increasing wollastonite content (Fig. 10). This indicates that the addition of wollastonite reduces the plastic deformation capability of the material.

Both $w_{e,y}$ and $w_{e,n}$ increase with increasing wollastonite content. However, increase in $w_{e,n}$ is more significant than in $w_{e,y}$. This indicates that the fracture toughness of PP–wollastonite–POE blends depends mainly on the post-yielding crack propagation resistance. The improvement in fracture toughness of the material through the addition of wollastonite is achieved by the improvement in the post-yielding crack propagation resistance of the materials.

The plastic deformation properties, βw_p, $\beta' w_{p,y}$, and $\beta'' w_{p,n}$, decrease with increasing wollastonite content. The value of $\beta' w_{p,y}$ is significantly larger than $\beta'' w_{p,n}$, indicating that the ability of plastic deformation of the material depends more on the pre-yielding properties.

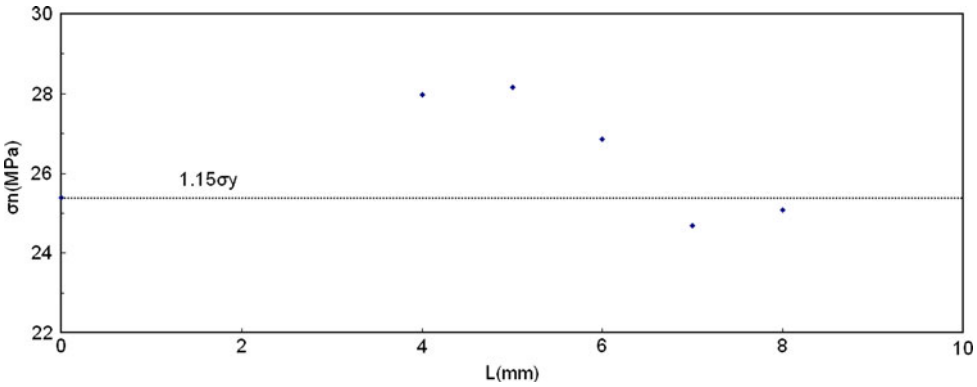

Fig. 3 Plots of the maximum net-section stress versus ligament length for PP–wollastonite–POE (82/10/8)

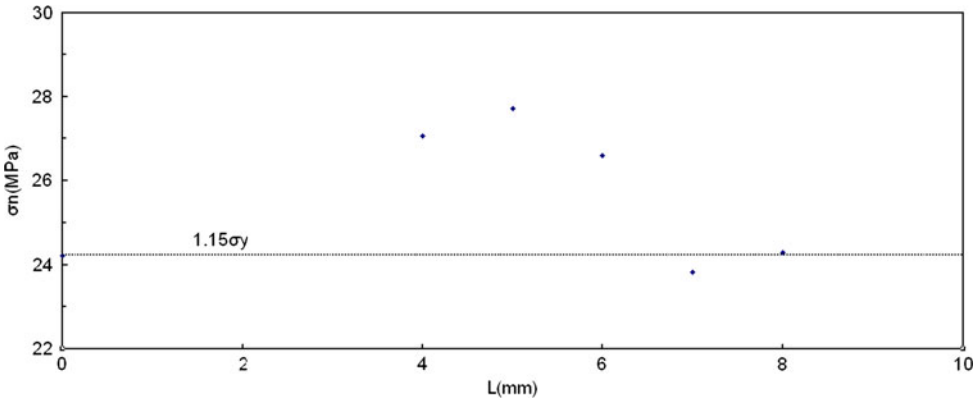

Fig. 4 Plots of the maximum net-section stress versus ligament length for PP–wollastonite–POE (72/20/8)

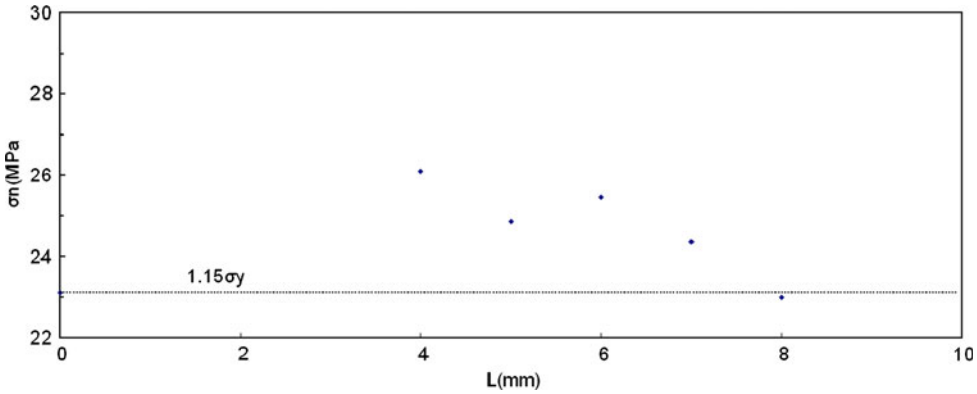

Fig. 5 Plots of the maximum net-section stress versus ligament length for PP–wollastonite–POE (62/30/8)

Impact strength

Figure 11 shows the impact strength of the PP–wollastonite–POE as a function of wollastonite content. The impact strength of pure PP is also presented for comparison.

It can be seen that the addition of POE improves the impact strength of the PP. The POE induces stresses and generates microcracks in the PP matrix. The stress fields of the microcracks interfere with each other, preventing them from forming macrocracks and improve the impact strength of the material [23].

However, introduction of wollastonite into PP–POE reduces the impact strength. At 30 wt% wollastonite, the impact strength is even lower than that of the pure PP. The wollastonite particles in the PP–POE serve as crack initiation sites. During impact strength test, these sites cause stress concentration and the impact strength to decrease. As the wollastonite content increases, the agglomeration of the particles increases, resulting in larger agglomerates (Figs. 14, 15), which leads to further reduction in impact strength.

Comparing Figs. 9 and 11, one can conclude that impact strength of a material may not correlate with its long-term

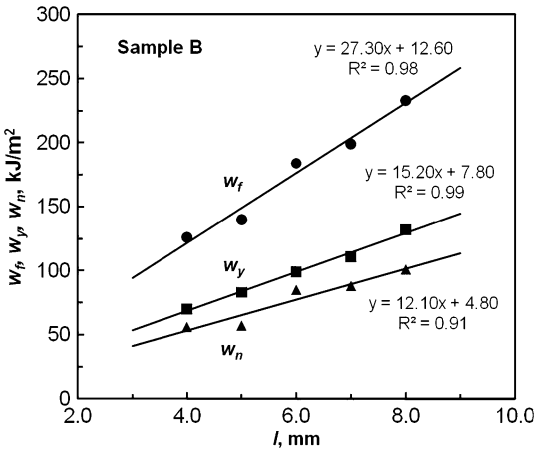

Fig. 6 w_f, w_y, and w_n of PP–wollastonite–POE (82/10/8) as function of ligament length

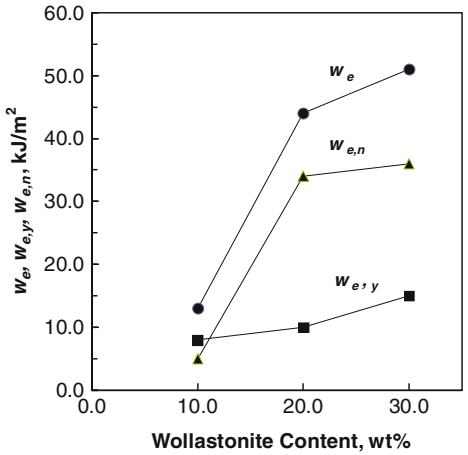

Fig. 9 w_e, $w_{e,y}$, and $w_{e,n}$ as a function of wollastonite content in the PP–wollastonite–8wt% POE system

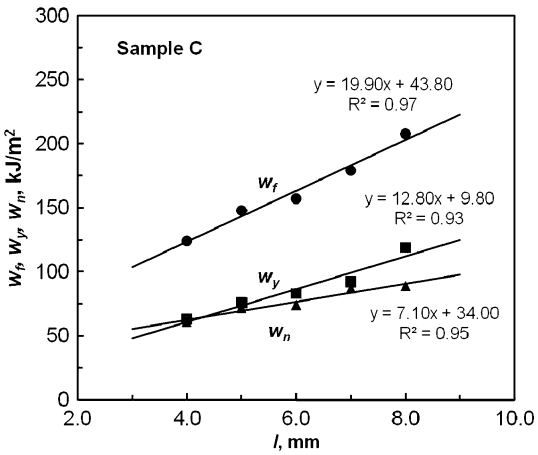

Fig. 7 w_f, w_y, and w_n of PP–wollastonite–POE (72/20/8) as function of ligament length

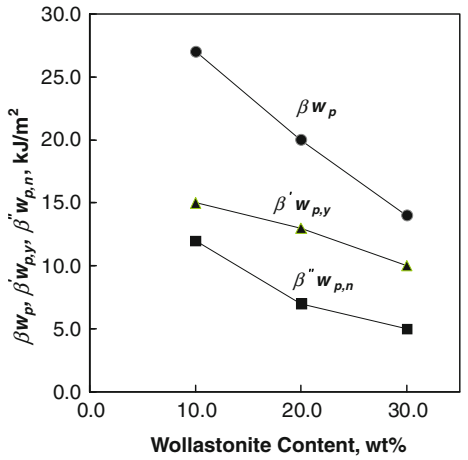

Fig. 10 βw_p, $\beta' w_{p,y}$, and $\beta'' w_{p,n}$ as function of wollastonite content in the PP–wollastonite–8wt% POE system

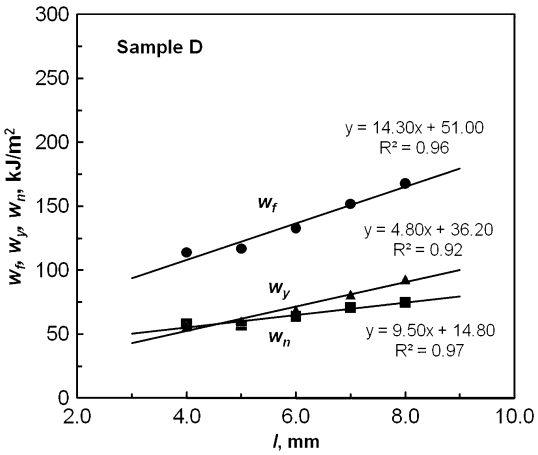

Fig. 8 w_f, w_y, and w_n of PP–wollastonite–POE (62/30/8) as function of ligament length

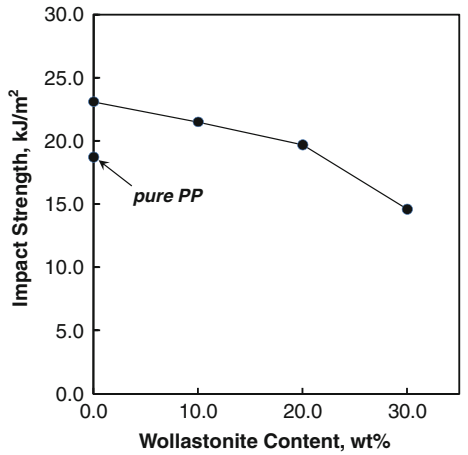

Fig. 11 Impact strength of PP–wollastonite–8wt% POE as function of wollastonite content

fracture properties. Materials with high impact strength can have low long-term fracture resistance.

Fracture surface morphology

Figures 12, 13, 14, and 15 show the fracture surfaces of the PP–wollastonite–POE. The fracture surfaces are quite rough, an indication of ductile fracture. Some of the wollastonite particles broke during the fracture process (Fig. 16), while others were pulled out, leaving voids in the matrix (Fig. 17). The pullout of the wollastonite particles from the matrix indicates the separation along the boundary between the wollastonite particle and the matrix during fracture. The ductility of the interface and the friction between the particles and the matrix dissipate fracture energy.

When the wollastonite content is small (sample B in Fig. 12), most particles disperse uniformly and bond well

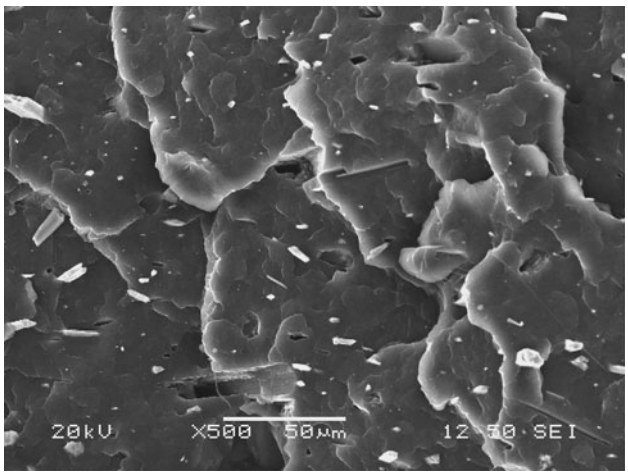

Fig. 12 Fracture surface of PP–wollastonite–POE (82/10/8)

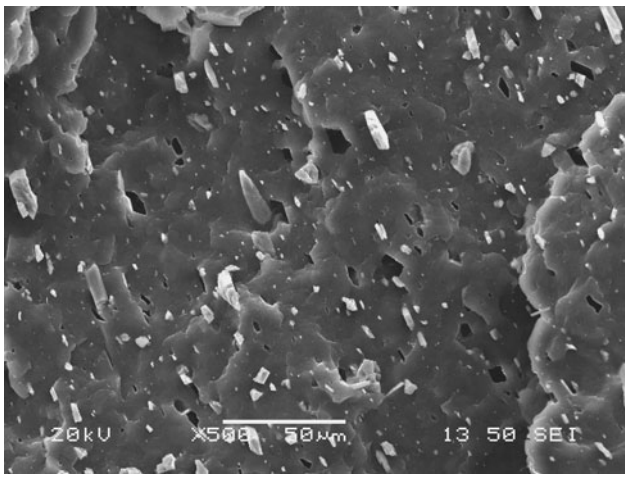

Fig. 13 Fracture surface of PP–wollastonite–POE (72/20/8)

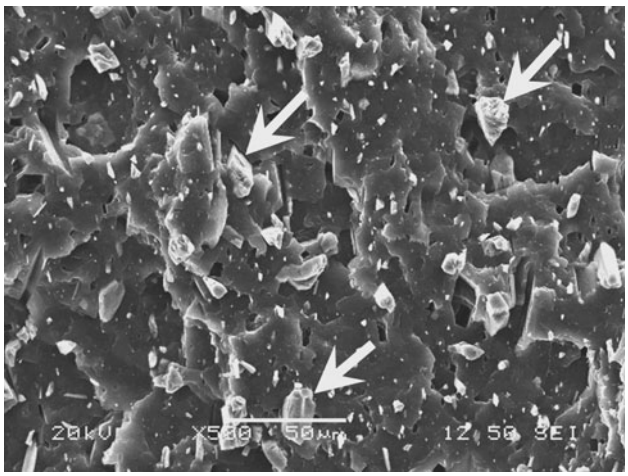

Fig. 14 Fracture surface of PP–wollastonite–POE (62/30/8) with wollastonite particles visible (arrows)

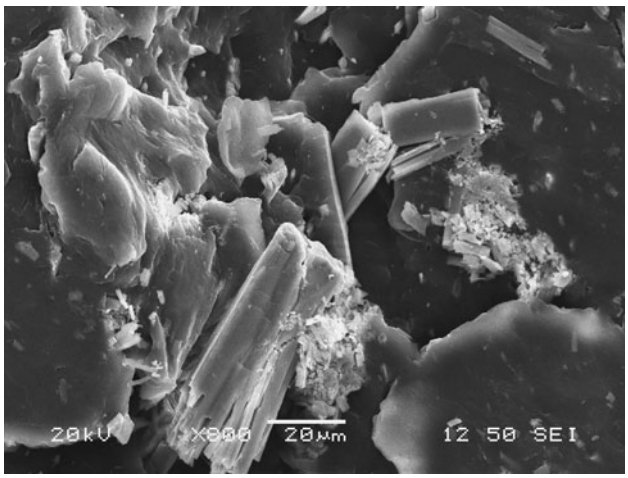

Fig. 15 Agglomerates of wollastonite in the PP–wollastonite–POE (72/20/8)

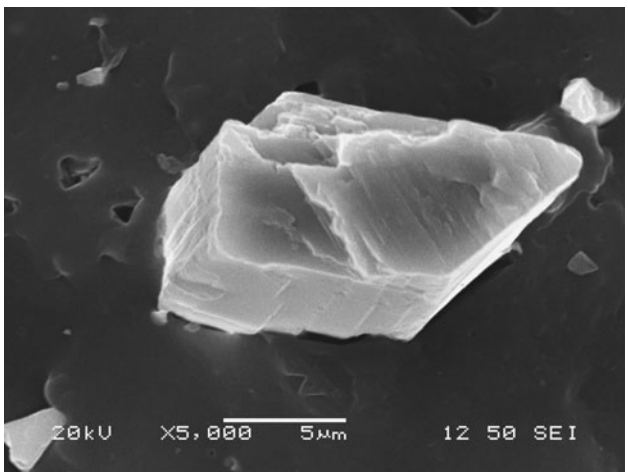

Fig. 16 A fractured wollastonite particle

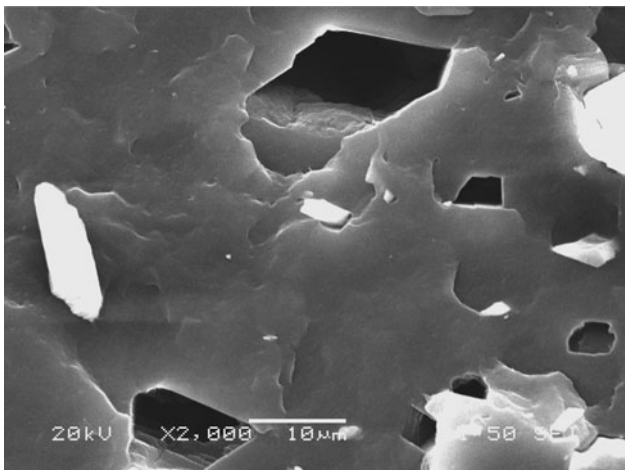

Fig. 17 The voids left behind by the pull out of wollastonite particles

with the matrix. They can transfer applied stresses to the matrix, causing large area plastic deformation and consuming more energy. As the wollastonite content become large, as seen in samples C and D (Figs. 13, 14), the particles start to form agglomerates (Figs. 14, 15), which have weaker bonding with the matrix. During the crack propagation, the agglomerates may be easily pulled out and leave voids behind (Fig. 17). The material fractures before it was fully plastically deformed and thus consumes less plastic deformation energy.

The change in w_e can be explained through the change in the microstructure of the material when wollastonite is introduced. When wollastonite disperses in the matrix as individual particles, they generate microcracks at surrounding matrix. Those cracks could interfere with each other during low speed crack propagation and thus increase the resistance to crack propagation, resulting in higher w_e of the material [24].

DSC analysis

Figure 18 is the melting curve of the PP–wollastonite–POE after the sample went through crystallization process at a constant cooling rate. Figure 19 shows the crystallization curves of the blends. Table 2 lists the DSC results where the crystallinity is calculated with the following equation [25]:

$$X_c = \left\{\Delta H_m / \left[(1-\eta)\Delta H_m^0\right]\right\} \times 100\%,$$

where ΔH_m is the melting enthalpy, ΔH_m^0 is the latent heat of fusion for 100% perfect crystals (209 J g^{-1} for PP), and η is the mass percentage of the filler.

The melting of the blends occurs around 165 °C (Fig. 18). The PP–wollastonite–POE composites have somewhat lower onset melting temperatures but higher peak melting temperature than the PP–POE.

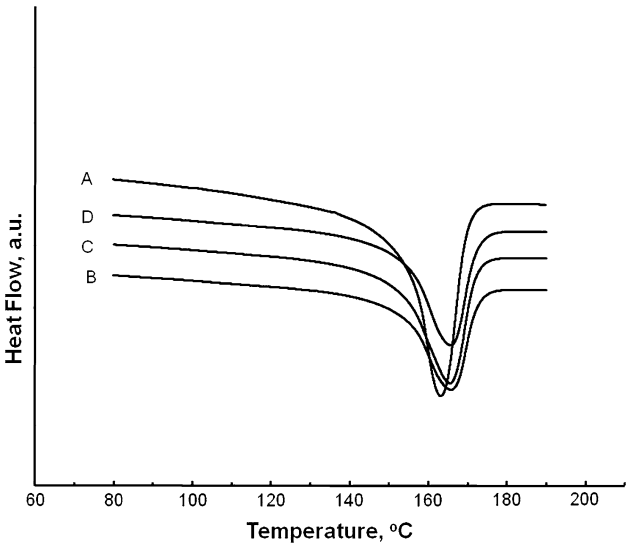

Fig. 18 The melting thermogram of PP–wollastonite–POE with various mass ratio: (*A*) 92/0/8; (*B*) 82/10/8; (*C*) 72/20/8; (*D*) 62/30/8

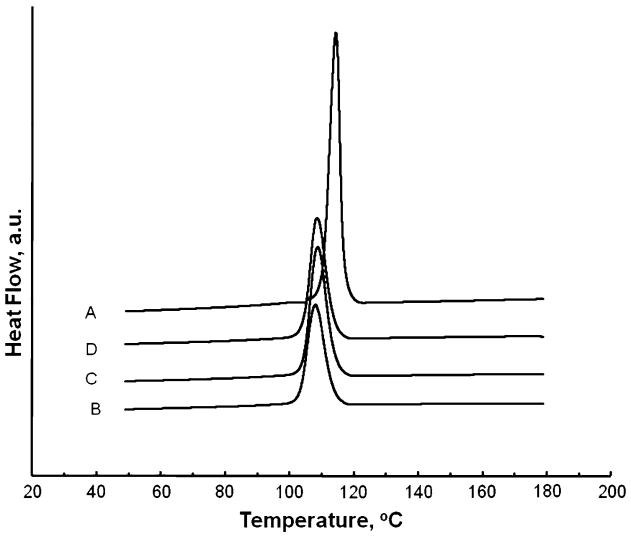

Fig. 19 The crystallization thermogram of PP–wollastonite–POE with various mass ratio: (*A*) 92/0/8; (*B*) 82/10/8; (*C*) 72/20/8; (*D*) 62/30/8

It can be seen from Table 2 that addition of wollastonite into PP–8wt% POE reduces the crystallinity and increases the overcooling ΔT_c. Among the PP–wollastonite–POE samples, sample C (mass ratio 72/20/8) has the highest crystallinity.

The addition of wollastonite increases the nucleation sites for the PP crystallization. However, the presence of the particles also limits the movement of the PP chains, making it difficult for the chains to fold to form crystals and reducing the available chains for crystallization. This reduces the crystallization rate, as reflected by the increase in ΔT_c. The effect of the second mechanism is stronger

Table 2 DSC results of PP–wollastonite–POE

Sample	$T_{m,onset}$ (°C)	$T_{m,peak}$ (°C)	ΔH_m (J g^{-1})	$T_{c,onset}$ (°C)	$T_{c,peak}$ (°C)	ΔT_c (°C)	ΔH_c (J g^{-1})	Xc (%)
A	154.6	163.1	84.0	116.8	114.4	48.7	98.8	44
B	153.3	165.8	49.2	113.7	108.0	57.8	56.2	30
C	151.6	165.5	51.3	114.1	108.7	56.8	56.7	34
D	153.4	165.6	38.7	113.9	108.8	56.9	45.0	31

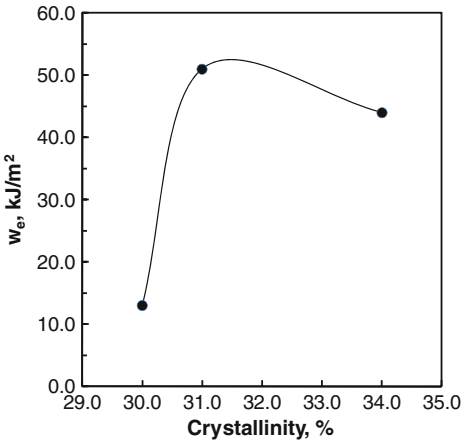

Fig. 20 Specific essential work of fracture (w_e) as a function of crystallinity in PP–wollastonite–8wt% POE

than that of the first [26, 27]. and the PP–wollastonite–POE has lower crystallinity than the PP–POE.

The crystallinity of sample C is higher than both samples B and D. Karger-Kocsis [8] suggested that as crystallinity increases, the crystalline lamellae becomes thicker and requires more energy to break, while the number of linking molecules and corresponding stress bearers decreases, reducing the toughness. These two opposite effects result in optimum fracture toughness at certain crystallinity. Figure 20 shows the specific essential work of fracture as a function of the crystallinity in the PP–wollastonite–POE. The fracture toughness has a maximum value as the crystallinity increases, in agreement with Karger-Kocsis' observation.

Conclusions

The effect of wollastonite content on the fracture properties of PP–wollastonite–POE composite in mixed-mode region was studied using EWF method. The DENT specimens of the composites showed typical ductile fracture. It was found in the mixed-mode that σ_n increases with shortening of the ligament length region as plastic constraint effect rises, and variation of the specific total work of fracture with ligament length was still reasonably linear within the mixed-mode region. The specific essential work of fracture w_e of the composites increases with increasing wollastonite content, while the specific non-essential work of fracture decreases, indicating the addition of wollastonite increases the crack propagation resistance while reduces the plastic deformation capability of the material. The fracture toughness of the composites depends mainly on the post-yielding crack propagation resistance of the material, while the plastic deformation capability is dependent on the pre-yielding behavior. The impact strength decreases with increasing wollastonite content. However, the composition with high impact strength has lower specific essential energy of fracture and lower long-term fracture resistance, indicating that EWF is a better indicator of long-term fracture properties than the impact strength. DSC results show that the presence of wollastonite hinders crystallization of the PP.

Acknowledgements The authors would like to acknowledge the support by the Hunan Provincial Natural Science Foundation of China (07JJ6016).

References

1. Tjong SC, Li RKY (1997) J Vinyl Add Technol 3:89
2. Fu SY et al (2002) J Mater Sci Eng A 323:326
3. Wang K, Wu J, Ye L, Zeng H (2003) Composites A 34:1199
4. Zhang L, Li C, Huang R (2005) J Polym Sci B 43:1113
5. Broberg KB (1975) J Mech Phys Solids 23:215
6. Mai YW, Cotterell B (1984) Int J Frac 24:229
7. Mai YW, Cotterell B (1986) Int J Frac 32:105
8. Karger-Kocsis J (1996) Polym Eng Sci 36:203
9. Karger-Kocsis J (1996) Polym Bull 36:119
10. Karger-Kocsis J (2000) In: Williams JG, Pavan A (eds), Fracture of polymers, composites and adhesives. ESIS Publication 28. Elsevier Science, Oxford, pp 213–230
11. Karger-Kocsis J (2002) In: Fakirov S (ed), Handbook of thermoplastic polyesters. Wiley-VCH, Weinheim, pp 717–753
12. Karger-Kocsis J, Bárány T (2002) Polym Eng Sci 42:1410
13. Hashemi S, Xu Y (2007) J Mater Sci 42:6197. doi:10.1007/s10853-006-1157-6
14. Ferrer-Balas D, Maspoch ML, Mai Y-W (2002) Polymer 43:3083
15. Ferrer-Balas D, Maspoch ML, Martinez AB, Santana OO (2001) Polymer 42:1697
16. Ben Jar P-Y, Adianto R (2009) Polym Eng Sci 50:530
17. Kwon HJ, Ben Jar P-Y (2006) Polym Eng Sci 46:1428
18. Levita G, Parisi L, Mcloughlin S (1996) J Mater Sci 31:1545. doi:10.1007/BF00357863
19. Hashemi S (1997) J Mater Sci 32:1563. doi:10.1007/BF00351217
20. Maspoch ML, Santana OO, Grando J (1997) Polym Bull 39:249

21. Karger-Kocsis J, Ferrer-Balas D (2001) Polym Bull 46:507
22. Wu J, Mai Y-W (1996) Polym Eng Sci 36:2275
23. Bucknall CB (1978) Adv Polym Sci 27:121
24. Grein C, Plummer CJG, Germain Y, Kausch HH, Béguelin P (2004) Polym Eng Sci 43:223
25. Van Krevelen DW, Holtyzer PJ (1976) Properties of polymers, their estimation and correlation with chemical structure. Elsevier Scientific, Amsterdam, p 620
26. Cheng Y, Xu M (1998) Acta Polym Sin 6:671
27. Jiang S, Ji X, An L, Jiang B (2000) Acta Polym Sin 4:452